Room Temperature Single-Photon Emission from Individual Perovskite Quantum Dots

Young-Shin Park,[†,‡] Shaojun Guo,[†] Nikolay S. Makarov,[†] and Victor I. Klimov*[,†]

[†]Chemistry Division, Los Alamos National Laboratory, Los Alamos, New Mexico 87545, United States and [‡]Center for High Technology Materials, University of New Mexico, Albuquerque, New Mexico 87131, United States

ABSTRACT Lead-halide-based perovskites have been the subject of numerous recent studies largely motivated by their exceptional performance in solar cells. Electronic and optical properties of these materials have been commonly controlled by varying the composition (*e.g.*, the halide component) and/or crystal structure. Use of nanostructured forms of perovskites can provide additional means for tailoring their functionalities *via* effects of quantum confinement and wave function engineering. Furthermore, it may enable applications that explicitly rely on the quantum nature of electronic excitations. Here, we demonstrate that $CsPbX_3$ quantum dots (X = I, Br) can serve as room-temperature sources of quantum light, as indicated by strong photon antibunching detected in single-dot photoluminescence measurements. We explain this observation by the presence of fast nonradiative Auger recombination, which renders multiexciton states virtually nonemissive and limits the fraction of photon coincidence events to ~6% on average. We analyze limitations of these quantum dots associated with irreversible photodegradation and fluctuations ("blinking") of the photoluminescence intensity. On the basis of emission intensity-lifetime correlations, we assign the "blinking" behavior to random charging/discharging of the quantum dot driven by photoassisted ionization. This study suggests that perovskite quantum dots hold significant promise for applications such as quantum emitters; however, to realize this goal, one must resolve the problems of photochemical stability and photocharging. These problems are largely similar to those of more traditional quantum dots and, hopefully, can be successfully resolved using advanced methodologies developed over the years in the field of colloidal nanostructures.

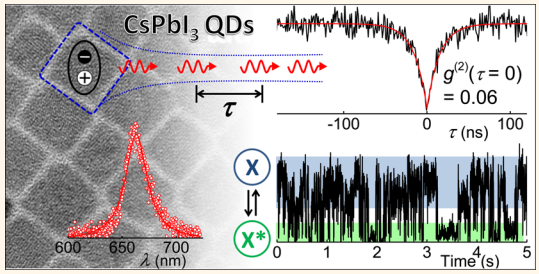

KEYWORDS: perovskite · quantum dot · nanocrystal · photoluminescence intermittency · blinking · photon antibunching · Auger recombination · photoionization

Perovskites have attracted considerable attention as a versatile materials platform for the realization of a new generation of solution-processable optoelectric devices including solar cells,[1−3] light-emitting diodes (LEDs),[4−6] and lasers.[7−9] The explosion of recent interest in these materials has been largely motivated by rapid advances in perovskite solar cells whose efficiencies skyrocketed from 3 to 4% in 2009[3] to ~20% in recent years.[2] In addition to exceptionally strong PV performance, perovskites have high emission quantum yields and composition-tunable emission wavelengths. These properties have been exploited in recent demonstrations of perovskite-based LEDs[4] and proof-of-principle lasing devices.[7−9] Several literature reports have presented colloidal synthesis of hybrid organic−inorganic ($CH_3NH_3PbX_3$)[10,11] and all-inorganic ($CsPbX_3$)[12] lead halide perovskite nanocrystals or quantum dots (QDs) with X = Cl, Br, I, and their mixtures. The use of nanostructured perovskite provides additional flexibility in tailoring their electronic and optical spectra by combining size and composition control, and also allows for the realization of principally new applications that explicitly rely on quantum-confined electronic excitations.

One particular application is a single-photon source (a "quantum emitter") which is a necessary element of quantum-information and quantum-communication schemes.[13,14] Epitaxially grown QDs have previously been used as quantum emitters under both optical and electrical excitation.[15,16] However, due to a fairly small separation between the quantized states, they operate in the single-photon mode only at cryogenic temperatures. Colloidal QDs offer a much greater degree of quantum confinement, which helps preserve the quantum character of

* Address correspondence to klimov@lanl.gov.

Received for review July 23, 2015 and accepted August 27, 2015.

Published online August 27, 2015
10.1021/acsnano.5b04584

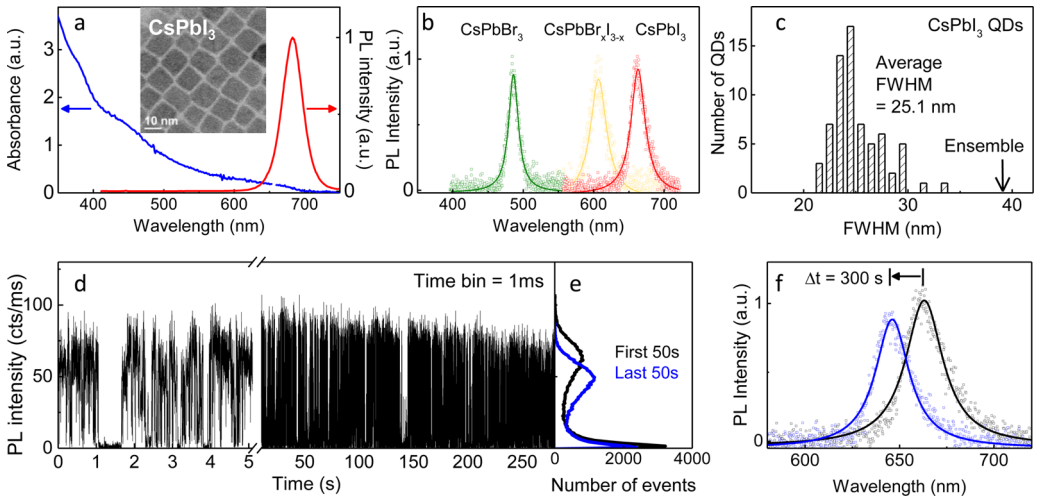

Figure 1. (a) Optical absorption (blue) and PL (red) spectra of $CsPbI_3$ perovskite QDs dispersed in hexane. The inset shows a TEM image. (b) Examples of single-dot PL spectra of $CsPbBr_3$ (green), $CsPbBr_xI_{3-x}$ (x = 1.3, yellow), and $CsPbI_3$ (red) QDs. (c) A FWHM histogram of 68 individual $CsPbI_3$ QDs. (d) The PL intensity trajectory and (e) the corresponding probability histogram recorded for a single $CsPbI_3$ quantum dot with 1 ms time bin using 488 nm cw excitation with I_p = 7.9 W/cm^2. (f) PL spectra of the same dot at the beginning (black) and the end (blue) of the measurements lasting for 300 s.

their emission at higher temperatures.[17] Even more importantly, multiphoton emission in this type of nanostructures is almost completely suppressed by extremely fast nonradiative Auger recombination, which renders multiexciton states virtually nonemissive.[18] This makes colloidal nanocrystals extremely robust quantum emitters independent of temperature or excitation intensity.

Here, we demonstrate that $CsPbX_3$-based perovskite QDs can serve as room-temperature sources of single photons. Specifically, we observe that emission from individual QDs exhibits strong photon antibunching under both continuous-wave (cw) and pulsed excitation with time-zero two-photon correlations of ~6% on average. As in the case of other known colloidal QDs, the antibunching arises from fast Auger recombination, which suppresses emission from biexcitons and other higher-order multiexcitons. We also examine deficiencies in these QDs associated with photoinduced degradation and photoluminescence (PL) intermittency ("blinking").[19] A comprehensive analysis of PL intensity and lifetime trajectories suggests that the PL blinking results from random charging/discharging of the QD driven by photoionization.

RESULTS AND DISCUSSION

We investigate $CsPbX_3$ QDs of different compositions ($CsPbBr_3$, $CsPbI_3$, and $CsPbBr_xI_{3-x}$ with x = 1.3 and 1.5) synthesized following the procedure from ref 12 with some modifications (see Methods). As indicated by transmission electron microscopy (TEM) measurements (inset of Figure 1a and Figure S1a of Supporting Information), these QDs have cubic shapes with mean sizes from 9.3 to 11.2 nm and a size dispersion of 8−10%. Examples of optical absorption and PL spectra of $CsPbBr_3$, $CsPbBr_xI_{3-x}$ and $CsPbI_3$ QDs dispersed in hexane are displayed in Figure 1a and Figure S1b. PL quantum yields (QYs) of these samples are from ~40% to ~50% (Figure S1b). For single-nanoparticle measurements,[20−23] a dilute solution of the QDs was mixed with a 3% solution of poly(methyl methacrylate) (PMMA) and spin coated onto a glass substrate. The QD areal density was kept below 0.1 μm^{-2} to allow for isolation of a single particle with a confocal microscope. The samples of $CsPbBr_xI_{3-x}$ and $CsPbI_3$ ($CsPbBr_3$) QDs were excited at 488 nm (405 nm) using either a cw or a pulsed (40 ps pulse width, 2 MHz repetition rate) laser. The emission from individual QDs was detected by silicon avalanche photodiodes and measured using a two-channel, time-tagged, time-correlated single photon counting (TCSPC) system with a temporal resolution of ~0.7 ns in pulsed measurements. In the case of pulsed excitation, the pump level was evaluated in terms of a nominal average QD excitonic occupancy calculated from $\langle N \rangle = j_p\sigma$, where j_p is the per-pulse photon fluence and σ is the QD absorption cross section (Figure S1b of Supporting Information). All data were collected at room temperature.

In Figure 1b, we show examples of single-dot PL spectra measured for $CsPbBr_3$, $CsPbBr_xI_{3-x}$ (x = 1.3), and $CsPbI_3$ QDs under cw excitation with an intensity (I_p) of ~10 W/cm^2. The spectral broadening evaluated in terms of a full width at half-maximum (FWHM, $\Delta\lambda_{1/2}$) is 17 nm ($CsPbBr_3$ QD), 28 nm ($CsPbBr_xI_{3-x}$ QD, x = 1.3), and 24 nm ($CsPbI_3$ QD), which is considerably narrower than the ensemble PL bandwidth (Figures 1a and S1b). The histogram of $\Delta\lambda_{1/2}$ for 68 individual $CsPbI_3$ dots is presented in Figure 1c. The majority of the QDs exhibit $\Delta\lambda_{1/2}$ between 20 and 30 nm with an average of 25.1 nm, again well below the PL linewidth measured for the ensemble QD solution ($\Delta\lambda_{1/2}$ = 38 nm, Figure 1a). These results suggest a considerable contribution of

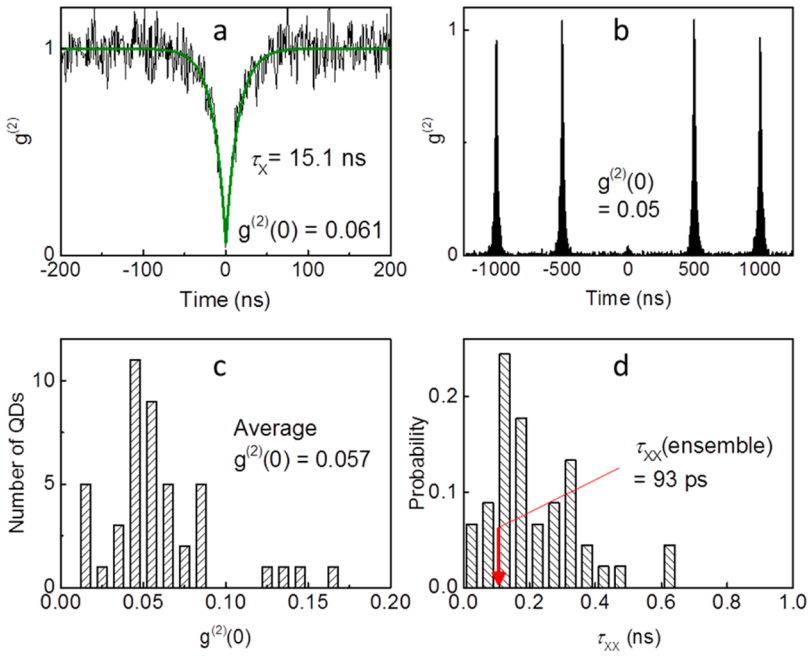

Figure 2. Second-order PL intensity correlation functions measured for a single $CsPbI_3$ QD under (a) cw (I_p = 7.9 W/cm^2) and (b) pulsed ($\langle N \rangle$ = 0.007) excitation. (c) Histogram of the $g^{(2)}(0)$ distribution based on the measurements of 45 QDs. (d) Probability histogram of the biexciton lifetime (τ_{XX}) derived from the measurements of the single-exciton lifetime (τ_X) and $g^{(2)}(0)$ from panel c.

size nonuniformity to the apparent PL bandwidth of QD ensemble samples.

A representative PL intensity trajectory of the individual $CsPbI_3$ QD recorded under cw excitation with I_p = 7.9 W/cm^2 is shown in Figure 1d. As was observed previously for other colloidal QDs,[19,24,25] the measured PL intensity fluctuates between two levels clearly resolved in the histogram in Figure 1e. The average signal from the low-emissivity (OFF) state is about 2 counts per millisecond (2 cts/ms), which is well above the background level of 0.36 cts/ms. The mean PL intensity during the high emissivity (ON) periods after the dot is freshly exposed to laser light is ~70 cts/ms. However, the count rate gradually decreases with time as evident from long time PL trajectories (right part of Figure 1d). On the basis of the PL intensity histograms in the example in Figure 1e, the ON state intensity decreases by ~23% during 300 s of QD exposure to laser light, which is accompanied by a *ca.* 16 nm blue shift of the PL peak (Figure 1f). These changes, which are enhanced with increasing pump intensity (see Figure S2), are typical signatures of photochemical degradation of the QDs.[26−28] The decrease in overall intensity is due to the creation of surface defects, acting as centers for nonradiative recombination, while the reduction of the semiconductor core of the QD leads to an increase of the band gap energy. These changes were permanent and could not be reversed, for example, by "resting" the sample in dark. Importantly, no signatures of degradation are observed without exposure to laser light (Figure S2a) indicating that it is a photoinduced process as was previously reported for other colloidal QDs.[26,27] We observe substantial dot-to-dot variations in the rate of photodegradation within the sample. The problem of photodegradation is even more severe with $CsPbBr_3$ and $CsPbBr_xI_{3-x}$ QDs. All of the tested dots of these compositions exhibit a significant PL loss during less than a minute of laser exposure (Figure S3).

Two-state, or "binary", PL blinking discussed above is strong evidence that single-dot emission is observed in our experiments. However, to confirm that a single dot acts as a source of quantum light, one needs to evaluate the statistical properties of the emitted stream of photons. To study PL photon statistics, we measure the second-order PL intensity correlation function, $g^{(2)}$, for individual $CsPbI_3$ QDs using a two-channel, Hanbury Brown and Twiss setup without spectral filtering of the emitted light.[29]

Figure 2a displays a two-photon cross-correlation trace normalized to its long-time amplitude recorded using cw excitation with intensity I_p = 7.9 W/cm^2. It shows that $g^{(2)}$ is only 0.06 at time t = 0 and then increases to unity at longer times. This is evidence of strong photon antibunching, a property of quantum emitters when photons are emitted one by one and the lag time between successive photon emission events is defined by the lifetime of the emitter's excited state. In the case of QDs, this is limited by the single-exciton lifetime (τ_X) which can be derived from the longer-time recovery of the $g^{(2)}$ signal, which yields τ_X = 15.1 ns based on the trace in Figure 2a. Strong antibunching is also observed for the perovskite QDs with pulsed excitation. In the example in Figure 2b, the magnitude

of the photon coincidence signal, $g^{(2)}(t = 0) = g^{(2)}(0)$, is ~0.05. The results of $g^{(2)}(0)$ measurements conducted on 45 QDs are summarized in Figure 2c. The majority of the studied dots showed $g^{(2)}(0)$ of less than 0.1 with an average of ~0.06. These results demonstrate that perovskite QDs do act as quantum emitters at room temperature with only a small parasitic background of ~6% on average.

In our measurements without spectral filtering of the collected PL, the time-zero photon coincidence signal arises from events when the QD is doubly excited (*i.e.*, is excited with a biexciton) and then emits two photons: one *via* the biexciton-to-exciton transition and the other *via* the exciton-to-ground-state transition. Hence, in the limit of low excitation fluences (when $\langle N \rangle \ll 1$), the amplitude of the antibunching peak is proportional to the product of the biexciton (Q_{XX}) and single-exciton (Q_X) PL QYs: $g^{(2)}(0) \propto Q_{XX}Q_X$.[22,23,30] On the other hand, the amplitude of the side peak observed in pulsed measurements [$g^{(2)}(T)$, where T is the pulse-to-pulse separation] scales as $(Q_X)^2$, because in the limit of $\langle N \rangle \rightarrow 0$, this peak arises from single-exciton emission events from two sequential excitation cycles. As a result, the area ratio of the $g^{(2)}$ central-to-side peaks measured at low pump intensities is equal to the ratio between biexciton and single-exciton PL QYs.[22,30] Since the condition $\langle N \rangle \ll 1$ is satisfied in all our photon correlation measurements, the value of $g^{(2)}(0)$ normalized by $g^{(2)}(T)$ provides a direct measure of Q_{XX}/Q_X.

Given our observations of strong antibunching [*i.e.*, nearly zero values of $g^{(2)}(0)$], the biexciton PL QY in perovskite QDs is very low. This is similar to the situation in standard (not specially "engineered") colloidal QDs of other compositions and is, as was discussed earlier, a direct consequence of a high nonradaitive Auger recombination rate which is much greater than the radiative rate. To estimate the biexciton lifetime (τ_{XX}) in perovskite QDs, we use the relationship $g^{(2)}(0) = Q_{XX}/Q_X$. We assume now that $g^{(2)}(0)$ is normalized by either the amplitude of a side peak (pulsed measurements) or the long time ($t \gg \tau_X$) $g^{(2)}$ signal (cw measurements). By expressing Q_{XX} and Q_X, in terms of full lifetimes of an exciton and a biexciton and their radiative lifetimes ($\tau_{r,X}$ and $\tau_{r,XX}$, respectively), we can rewrite the expression for $g^{(2)}(0)$ as $g^{(2)}(0) = (\tau_{r,X}/\tau_{r,XX})(\tau_{XX}/\tau_X)$, or $g^{(2)}(0) = 4\tau_{XX}/\tau_X$ if we assume the usual quadratic scaling of radiative rates with exciton multiplicity.[31]

By applying the previous expression to the data in Figure 2c, we can extract τ_{XX} on the basis of the measured $g^{(2)}(0)$ and τ_X. The resultant data are presented as a probability histogram in Figure 2d. The peak of the probability corresponds to τ_{XX} of ~100 ps, which is close to the value of 93 ps obtained from time-resolved ensemble measurements of the solution sample (Figure S4a–c). As in the case of other colloidal nanocrystals, extremely short values of τ_{XX} in perovskite QDs result from fast nonradiative Auger decay which leads to essentially complete suppression of the photon coincidence signal in the $g^{(2)}$ measurements and explains our observation of strong photon antibunching in the emitted light.

While photon correlation studies indicate potential applicability of perovskite QDs as single-photon emitters, strong emission intermittency (Figure 1d) complicates practical implementation of this type of technology. To develop a solution to this problem, it is important to elucidate the mechanism underlying PL blinking. Several recent studies of hybrid organometallic perovskite particles also indicated fluctuations of the PL intensity.[32−35] The observed behaviors as well as proposed explanations differed considerably from one report to another. For example, larger micrometer-scale particles[32] were observed to exhibit rare OFF periods, however, the PL was affected across the entire crystal. This behavior was referred to as "synchronous blinking" and compared to that previously observed, for example, in long CdSe nanowires.[36] Submicrometer perovskite particles investigated in ref 34 exhibited large-amplitude ("giant") blinking with multiple intensity levels, which was attributed to the existence of a small number of either "quenching" or "emitting" sites to which excitations generated across the whole particle were funneled. A study of electronically coupled submicrometer perovskite crystals[33] also reported PL blinking; however, it was interpreted not in terms of spatially localized quenchers/emitters but rather Auger recombination of photogenerated carriers with pre-existing charges trapped at the particle interfaces. The involvement of surface/interface traps was also invoked in ref 35 to explain PL blinking of fairly small but highly polydisperse (10−50 nm size) perovskite particles.

The above survey indicates a wide diversity of observed PL blinking patterns as well as proposed blinking models. The insights gained from these studies, however, are not likely applicable to our nanocrystals as most of the previous works have investigated bulk-like structures that did not exhibit pronounced quantum confinement. For example, the lack of photon antibunching in measurements of ref 33 directly pointed to the fact that the studied particles were too large to exhibit properties of quantum emitters. This is in contrast to strong photon antibunching revealed by our measurements of quantum confined perovskite nanocrystals.

The smallest particle sizes probed previously by single-particle spectroscopy were 10−50 nm.[35] However, even in that case the observed blinking behaviors were quite distinct from those seen in our experiments. Specifically, the measurements of ref 35 showed multiple PL intensity levels and pronounced photobrightening, while our studies reveal two well-defined emission

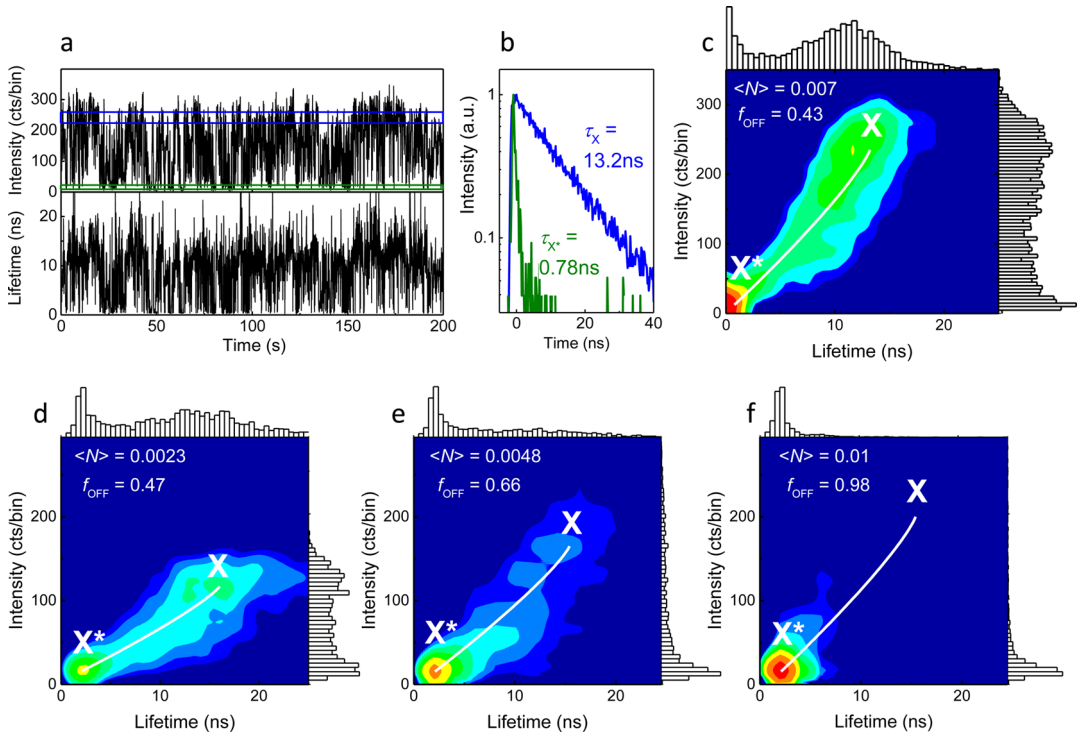

Figure 3. (a) PL intensity (upper panel) and lifetime (lower panel) trajectories for a single $CsPbI_3$ QD measured using 488 nm pulsed excitation (2 MHz repetition rate) with $\langle N \rangle = 0.007$ and bin size of 50 ms. (b) PL decay of the ON (blue) and OFF (green) states obtained by collecting emission with intensities from the two intervals shown in panel a by horizontal lines of corresponding colors. (c) A false color representation of FLID obtained from the analysis of I_{PL} and τ_{PL} in panel a. A color change from blue to red corresponds to increasing probability of occurrence of a given state in the $I_{PL}-\tau_{PL}$ space. The white line is a charging trajectory obtained according to the procedure described in the Supporting Information (Section 5). The I_{PL} and τ_{PL} probability histograms are shown along the horizontal (top) and the vertical (right) FLID axes, respectively. (d and e) Pump-fluence dependence of FLIDs obtained for $\langle N \rangle = 0.0023$, 0.0048, and 0.01 (shown in the corresponding panels).

levels and gradual PL quenching under prolonged illumination. This suggests that underlying physics of PL blinking in our samples is different from that in ref 35.

To gain a deeper insight into the mechanism for PL intermittency in our QDs, we analyze correlations between fluctuations of the PL intensity (I_{PL}) and PL lifetime (τ_{PL}) using time-tagged TCSPC measurements with pulsed excitation. The inspection of PL intensity and lifetime trajectories (Figure 3a) immediately indicates the existence of a direct correlation between these quantities, which is especially pronounced in a fluorescence-lifetime-intensity-distribution (FLID) plot (Figure 3c) where the likelihood of the dot to occupy a certain state in the "I_{PL}-τ_{PL} space" is shown by false color changing from blue to red with increasing probability. The blinking trajectories along with the FLID indicate that the drop in the PL intensity is accompanied by a simultaneous shortening of the PL lifetime. According to the classification in ref 37, this is a signature of type-A blinking as opposed to type-B blinking where fluctuations of I_{PL} occur without considerable changes in τ_{PL}.

In the case of traditional colloidal QDs, type-A blinking is usually associated with fluctuations between a neutral (ON) and a charged (OFF) exciton state. The reduced PL QY of the charged exciton (trion) is due to fast nonradiative Auger decay discussed earlier in the context of two-photon correlation measurements. As we elaborate below, a similar A-type charging/discharging mechanism is likely responsible for the observed PL blinking of perovskite QDs. The PL dynamics measured for high and low-emissivity states (Figure 3b) indicate that their lifetimes are 13.2 ns (τ_{ON}) and 0.78 ns (τ_{OFF}). Within the charging/discharging model these lifetimes should be attributed to the neutral exciton (X) and the trion (X*), respectively. The former of these values is nearly the same as the time constant inferred from the cw $g^{(2)}$ measurements (Figure 2a), in which it was assigned to the single-exciton decay, in agreement with the present assignment. Unfortunately, the OFF-state lifetime is resolution limited and, thus, not specific enough to make its exact assignment.

For a more accurate determination of τ_{OFF}, we compare the intensities of the ON ($I_{ON,PL}$) and the OFF ($I_{OFF,PL}$) levels, and then infer τ_{OFF} from the expression $\tau_{OFF} = (\tau_{ON}/\eta)(I_{OFF,PL}/I_{ON,PL})$, where η is the ratio between the radiative rates of the OFF and the ON states. From the PL intensity histograms in Figure 3c, the $I_{OFF,PL}/I_{ON,PL}$ ratio is around 0.03. If we assume that the OFF periods are due to QD charging, then η is equal to 2 as the presence of an extra carrier in the dot

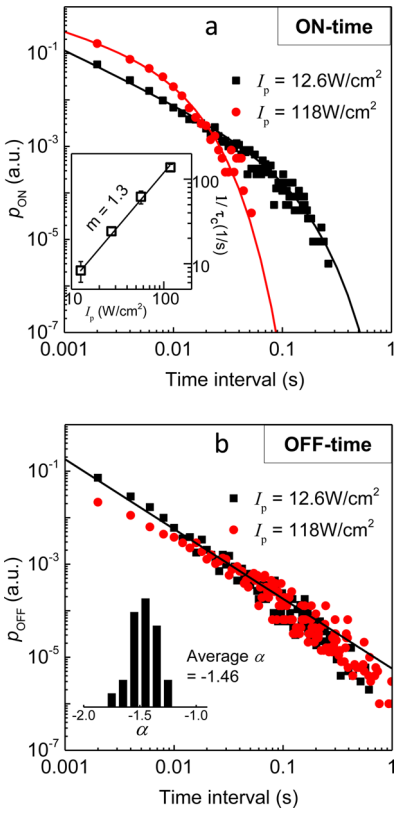

Figure 4. Probability distributions of (a) the ON-times and (b) the OFF-times plotted in the log−log representation. Inset in (a) shows $1/\tau_C$ as a function of pump intensity (symbols) along with a fit to I_p^m (line). Inset in (b) displays the probability histogram of the OFF-time exponent.

doubles the number of radiative pathways.[31] When we use τ_{ON} = 13.2 ns (Figure 3b), we obtain τ_{OFF} of 200 ps. To estimate the trion lifetime (τ_{X^*}), we can use the relationship $2\tau_{XX} \leq \tau_{X^*} \leq 4\tau_{XX}$, if we assume that the trion decay is dominated by Auger recombination.[31,38] Using τ_{XX} of ∼90 ps from the earlier discussion, we obtain 180 ps ≤ τ_{X^*} ≤ 360 ps, which indicates that τ_{OFF} is in the range of lifetimes expected for trion Auger decay.

Further evidence in favor of the charging/discharging model comes from the analysis of pump-intensity dependent FLIDs (Figure 3d−f). It indicates that the increase in the pump intensity leads to increased fraction of time (f_{OFF}) the QD spends in the OFF state (see Section 5 of Supporting Information for derivation of f_{OFF}). Specifically, according to FLIDs in Figure 3d−f, f_{OFF} progressively increases from 0.47 to 0.66 and then 0.98 when ⟨N⟩ changes from 0.0023 to 0.0048 and finally 0.01. This behavior is reversible, and therefore, is *not* due to permanent photodegradation but rather due to photoassisted charging (photoionization) as was observed previously for II−VI QDs.[24,25,37,39]

A known fingerprint of photoionization in QD blinking studies is an exponential cutoff in the distribution of the PL ON-time periods (t_{ON}), where the cutoff time (τ_C) is directly linked to the pump intensity.[37,40] We indeed observe this truncation behavior in our measurements. In Figure 4, we display the probability distributions of the ON (p_{ON}, panel a) and OFF (p_{OFF}, panel b) time periods derived from the PL intensity trajectories measured using cw excitation with intensities 12.6 W/cm^2 (black squares) and 118 W/cm^2 (red circles). In the log−log representation used in the plot, the OFF-time probability distribution shows an essentially linear behavior, which is a signature of a power-law dependence, $p_{OFF} \propto t^{\alpha}$ (α = −1.46 on average), commonly observed in previous blinking studies of II−VI QDs.[41,42] The distribution of p_{ON} is qualitatively different and shows a rapid falloff at longer times, which can be described by $p_{ON} \propto t^{\beta} \exp(-t/\tau_C)$ with β = −1.2 (− 0.66) and τ_C = 120 ms (7.3 ms) for I_p = 12.6 W/cm^2 (118 W/cm^2). Similar statistics of the ON- and OFF-time probabilities have also been observed for $CsPbBr_3$ and $CsPbBr_xI_{3-x}$ QDs (Figure S6). As expected when the duration of ON-time periods is limited by photoionization, τ_C is pump intensity dependent. Specifically, according to our measurements (inset of Figure 4a), $1/\tau_C$ shows an increase with I_p following an I_p^m dependence with m of ∼1.3.

Analogous trends were previously reported for CdSe/CdS QDs, which were interpreted and quantitatively modeled assuming that QD charging is a photo-assisted process.[40−45] The probability of photoionization ($p_{ion} \propto 1/\tau_C$) has been observed to exhibit both linear[40,42,44] and superlinear (*e.g.*, quadratic)[43] dependence on pump power with the latter being usually attributed to Auger ionization. Our measurements of τ_C (inset of Figure 4a) indicate that p_{ion} is superlinear in pump intensity ($p_{ion} \propto I_p^{1.3}$), suggesting that in perovskite QDs both linear and nonlinear (such as Auger ionization) processes likely contribute to QD photocharging.

CONCLUSIONS

To summarize, single-particle measurements of perovskite $CsPbX_3$ (X = I, Br) QDs indicate that they are quantum emitters at room temperature; that is, they show strong photon antibunching of the emitted light. We also observed strong fluctuations in the PL intensity that correlate with fluctuations of the PL lifetime. This behavior is typical of "A-type blinking"[37] which is usually associated with the fluctuation of the QD charge when the ON and the OFF states are ascribed to a neutral and a charged exciton, respectively. The analysis of blinking trajectories as a function of excitation intensity suggests that charging is driven by photoionization due to a combination of both linear and nonlinear (in pump intensity) processes.

Interestingly, the PL blinking behaviors observed in the present study are notably different from those reported previously for larger-size perovskite nanostructures.[32−35] However, if we analyze our results in the context of previous work on more traditional colloidal QDs (based, *e.g.*, on II−VI semiconductors), we find many similarities. This provides yet another

example of the generality of many physical phenomena across strongly confined colloidal nanocrystals of different compositions. In addition to PL blinking, colloidal QDs exhibit remarkably similar trends in intraband relaxation, Auger recombination, magneto-optical properties, *etc*. One might expect that at least some of these trends also apply to the emerging class of QDs based on perovskites, and thus, a vast amount of previous work on colloidal nanocrystals may provide useful insights into physical behaviors of these novel materials.

The lessons learned from studies of colloidal nanostructures may also be helpful in tackling the problem of environmental- and photostability of perovskites materials. Our observation of the extreme propensity of perovskite QDs to photodegrade, in connection with previously published work, suggests that this problem is general to both bulk and nanostructured forms of these materials. The field of colloidal QDs has successfully resolved the problem of instability for many types of extremely sensitive nanomaterials, including Pb-based structures. Some of these advanced methodologies can hopefully be applied to perovskite nanostructures, helping to advance this field in the direction of practical technologies.

METHODS

Chemicals and Materials. Oleic acid (OA, 90%), octadecene (ODE), oleylamine (OAm, 80−90%), Cs_2CO_3, hexane, PbI_2, and $PbBr_2$ were purchased from Aldrich. All chemicals were used as received without any further purification.

Synthesis of $CsPbX_3$ QDs. For the synthesis of Cs-oleate, 0.8 g of Cs_2CO_3 was loaded into a mixture of 30 mL of octadecene and 2.5 mL of oleic acid, and then heated to 200 °C until the white power was completely dissolved. Then, the mixture was kept at 130 °C for 1 h under vacuum. Note that during the synthesis of perovskite QDs, the temperature of Cs−oleate mixture should be kept at least at 130 °C to avoid precipitation. For the synthesis of the $CsPbI_3$ QDs, 0.092 g of PbI_2 was added into a mixture of 5 mL of ODE, 0.5 mL of OAm and 0.5 mL of OA, and then heated to 120 °C for 30 min under vacuum. The temperature was then raised to 180 °C, followed by the rapid injection of 0.45 mL of Cs−oleate solution, and then the solution was rapidly cooled by the water bath. The synthesis of $CsPbBr_3$ and $CsPbBr_xI_{3-x}$ (x = 1.3) QDs was conducted using the same protocol but replacing the PbI_2 precursor with, respectively, $PbBr_2$ (0.072 g) or a mixture of PbI_2 (0.046 g) and $PbBr_2$ (0.036 g).

Conflict of Interest: The authors declare no competing financial interest.

Acknowledgment. These studies were supported by the Chemical Sciences, Biosciences and Geosciences Division, Office of Basic Energy Sciences, Office of Science, U.S. Department of Energy.

Supporting Information Available: The Supporting Information is available free of charge on the ACS Publications website at DOI: 10.1021/acsnano.5b04584.

Absorption and PL spectra, measurements of irreversible photodegradation, PL blinking of individual $CsPbBr_3$ and $CsPbBr_xI_{3-x}$ QDs, pump-intensity dependence of PL dynamics for the $CsPbI_3$ QD solution sample, quantitative analysis of photocharging, ON- and OFF-time probability distributions for $CsPbBr_3$ and $CsPbBr_xI_{3-x}$ QDs (PDF)

REFERENCES AND NOTES

1. Green, M. A.; Ho-Baillie, A.; Snaith, H. J. The Emergence of Perovskite Solar Cells. *Nat. Photonics* **2014**, *8*, 506–514.
2. Zhou, H.; Chen, Q.; Li, G.; Luo, S.; Song, T.-b.; Duan, H.-S.; Hong, Z.; You, J.; Liu, Y.; Yang, Y. Interface Engineering of Highly Efficient Perovskite Solar Cells. *Science* **2014**, *345*, 542–546.
3. Kojima, A.; Teshima, K.; Shirai, Y.; Miyasaka, T. Organometal Halide Perovskites as Visible-Light Sensitizers for Photovoltaic Cells. *J. Am. Chem. Soc.* **2009**, *131*, 6050–6051.
4. Li, G.; Tan, Z.-K.; Di, D.; Lai, M. L.; Jiang, L.; Lim, J. H.-W.; Friend, R. H.; Greenham, N. C. Efficient Light-Emitting Diodes Based on Nanocrystalline Perovskite in a Dielectric Polymer Matrix. *Nano Lett.* **2015**, *15*, 2640–2644.
5. Kim, Y.-H.; Cho, H.; Heo, J. H.; Kim, T.-S.; Myoung, N.; Lee, C.-L.; Im, S. H.; Lee, T.-W. Multicolored Organic/Inorganic Hybrid Perovskite Light-Emitting Diodes. *Adv. Mater.* **2015**, *27*, 1248–1254.
6. Tan, Z.-K.; Moghaddam, R. S.; Lai, M. L.; Docampo, P.; Higler, R.; Deschler, F.; Price, M.; Sadhanala, A.; Pazos, L. M.; Credgington, D.; et al. Bright Light-Emitting Diodes Based on Organometal Halide Perovskite. *Nat. Nanotechnol.* **2014**, *9*, 687–692.
7. Zhu, H.; Fu, Y.; Meng, F.; Wu, X.; Gong, Z.; Ding, Q.; Gustafsson, M. V.; Trinh, M. T.; Jin, S.; Zhu, X. Y. Lead Halide Perovskite Nanowire Lasers with Low Lasing Thresholds and High Quality Factors. *Nat. Mater.* **2015**, *14*, 636–643.
8. Zhang, Q.; Ha, S. T.; Liu, X.; Sum, T. C.; Xiong, Q. Room-Temperature Near-Infrared High-Q Perovskite Whispering-Gallery Planar Nanolasers. *Nano Lett.* **2014**, *14*, 5995–6001.
9. Xing, G.; Mathews, N.; Lim, S. S.; Yantara, N.; Liu, X.; Sabba, D.; Grätzel, M.; Mhaisalkar, S.; Sum, T. C. Low-Temperature Solution-Processed Wavelength-Tunable Perovskites for Lasing. *Nat. Mater.* **2014**, *13*, 476–480.
10. Zhang, F.; Zhong, H.; Chen, C.; Wu, X.-g.; Hu, X.; Huang, H.; Han, J.; Zou, B.; Dong, Y. Brightly Luminescent and Color-Tunable Colloidal $CH_3NH_3PbX_3$ (X = Br, I, Cl) Quantum Dots: Potential Alternatives for Display Technology. *ACS Nano* **2015**, *9*, 4533–4542.
11. Schmidt, L. C.; Pertegás, A.; González-Carrero, S.; Malinkiewicz, O.; Agouram, S.; Mínguez Espallargas, G.; Bolink, H. J.; Galian, R. E.; Pérez-Prieto, J. Nontemplate Synthesis of $CH_3NH_3PbBr_3$ Perovskite Nanoparticles. *J. Am. Chem. Soc.* **2014**, *136*, 850–853.
12. Protesescu, L.; Yakunin, S.; Bodnarchuk, M. I.; Krieg, F.; Caputo, R.; Hendon, C. H.; Yang, R. X.; Walsh, A.; Kovalenko, M. V. Nanocrystals of Cesium Lead Halide Perovskites ($CsPbX_3$, X = Cl, Br, and I): Novel Optoelectronic Materials Showing Bright Emission with Wide Color Gamut. *Nano Lett.* **2015**, *15*, 3692–3696.
13. Bennett, C. H.; DiVincenzo, D. P. Quantum Information and Computation. *Nature* **2000**, *404*, 247–255.
14. Gisin, N.; Ribordy, G.; Tittel, W.; Zbinden, H. Quantum Cryptography. *Rev. Mod. Phys.* **2002**, *74*, 145.
15. Santori, C.; Pelton, M.; Solomon, G.; Dale, Y.; Yamamoto, Y. Triggered Single Photons from a Quantum Dot. *Phys. Rev. Lett.* **2001**, *86*, 1502–1505.
16. Yuan, Z.; Kardynal, B. E.; Stevenson, R. M.; Shields, A. J.; Lobo, C. J.; Cooper, K.; Beattie, N. S.; Ritchie, D. A.; Pepper, M. Electrically Driven Single-Photon Source. *Science* **2002**, *295*, 102–105.
17. Michler, P.; Imamoglu, A.; Mason, M. D.; Carson, P. J.; Strouse, G. F.; Buratto, S. K. Quantum Correlation among Photons from a Single Quantum Dot at Room Temperature. *Nature* **2000**, *406*, 968–970.
18. Klimov, V. I.; Mikhailovsky, A. A.; McBranch, D. W.; Leatherdale, C. A.; Bawendi, M. G. Quantization of Multiparticle Auger Rates in Semiconductor Quantum Dots. *Science* **2000**, *287*, 1011–1013.

19. Efros, A. L.; Rosen, M. Random Telegraph Signal in the Photoluminescence Intensity of a Single Quantum Dot. *Phys. Rev. Lett.* **1997**, *78*, 1110–1113.
20. Jin, S.; Song, N.; Lian, T. Suppressed Blinking Dynamics of Single QDs on ITO. *ACS Nano* **2010**, *4*, 1545–1552.
21. Osovsky, R.; Cheskis, D.; Kloper, V.; Sashchiuk, A.; Kroner, M.; Lifshitz, E. Continuous-Wave Pumping of Multiexciton Bands in the Photoluminescence Spectrum of a Single CdTe-CdSe Core-Shell Colloidal Quantum Dot. *Phys. Rev. Lett.* **2009**, *102*, 197401.
22. Park, Y.-S.; Malko, A. V.; Vela, J.; Chen, Y.; Ghosh, Y.; Garcia-Santamar, F.; Hollingsworth, J. A.; Klimov, V. I.; Htoon, H. Near-Unity Quantum Yields of Biexciton Emission from CdSe/CdS Nanocrystals Measured Using Single-Particle Spectroscopy. *Phys. Rev. Lett.* **2011**, *106*, 187401.
23. Park, Y.-S.; Bae, W. K.; Padilha, L. A.; Pietryga, J. M.; Klimov, V. I. Effect of the Core/Shell Interface on Auger Recombination Evaluated by Single-Quantum-Dot Spectroscopy. *Nano Lett.* **2014**, *14*, 396–402.
24. Malko, A. V.; Park, Y.-S.; Sampat, S.; Galland, C.; Vela, J.; Chen, Y.; Hollingsworth, J. A.; Klimov, V. I.; Htoon, H. Pump-Intensity- and Shell-Thickness-Dependent Evolution of Photoluminescence Blinking in Individual Core/Shell CdSe/CdS Nanocrystals. *Nano Lett.* **2011**, *11*, 5213–5218.
25. Nirmal, M.; Dabbousi, B. O.; Bawendi, M. G.; Macklin, J. J.; Trautman, J. K.; Harris, T. D.; Brus, L. E. Fluorescence Intermittency in Single Cadmium Selenide Nanocrystals. *Nature* **1996**, *383*, 802–804.
26. Hines, D. A.; Becker, M. A.; Kamat, P. V. Photoinduced Surface Oxidation and Its Effect on the Exciton Dynamics of CdSe Quantum Dots. *J. Phys. Chem. C* **2012**, *116*, 13452–13457.
27. van Sark, W. G. J. H. M.; Frederix, P. L. T. M.; Van den Heuvel, D. J.; Gerritsen, H. C.; Bol, A. A.; van Lingen, J. N. J.; de Mello Donegá, C.; Meijerink, A. Photooxidation and Photobleaching of Single CdSe/ZnS Quantum Dots Probed by Room-Temperature Time-Resolved Spectroscopy. *J. Phys. Chem. B* **2001**, *105*, 8281–8284.
28. Sykora, M.; Koposov, A. Y.; McGuire, J. A.; Schulze, R. K.; Tretiak, O.; Pietryga, J. M.; Klimov, V. I. Effect of Air Exposure on Surface Properties, Electronic Structure, and Carrier Relaxation in PbSe Nanocrystals. *ACS Nano* **2010**, *4*, 2021–2034.
29. Brown, R. H.; Twiss, R. Q. Correlation between Photons in two Coherent Beams of Light. *Nature* **1956**, *177*, 27–29.
30. Nair, G.; Zhao, J.; Bawendi, M. G. Biexciton Quantum Yield of Single Semiconductor Nanocrystals from Photon Statistics. *Nano Lett.* **2011**, *11*, 1136–1140.
31. Klimov, V. I. Multicarrier Interactions in Semiconductor Nanocrystals in Relation to the Phenomena of Auger Recombination and Carrier Multiplication. *Annu. Rev. Condens. Matter Phys.* **2014**, *5*, 285–316.
32. Zhu, F.; Men, L.; Guo, Y. J.; Zhu, Q. C.; Bhattacharjee, U.; Goodwin, P. M.; Petrich, J. W.; Smith, E. A.; Vela, J. Shape Evolution and Single Particle Luminescence of Organometal Halide Perovskite Nanocrystals. *ACS Nano* **2015**, *9*, 2948–2959.
33. Wen, X.; Ho-Baillie, A.; Huang, S.; Sheng, R.; Chen, S.; Ko, H.-c.; Green, M. A. Mobile Charge-Induced Fluorescence Intermittency in Methylammonium Lead Bromide Perovskite. *Nano Lett.* **2015**, *15*, 4644–4649.
34. Tian, Y.; Merdasa, A.; Peter, M.; Abdellah, M.; Zheng, K.; Ponseca, C. S.; Pullerits, T.; Yartsev, A.; Sundström, V.; Scheblykin, I. G. Giant Photoluminescence Blinking of Perovskite Nanocrystals Reveals Single-Trap Control of Luminescence. *Nano Lett.* **2015**, *15*, 1603–1608.
35. Tachikawa, T.; Karimata, I.; Kobori, Y. Surface Charge Trapping in Organolead Halide Perovskites Explored by Single-Particle Photoluminescence Imaging. *J. Phys. Chem. Lett.* **2015**, *6*, 3195–3201.
36. Glennon, J. J.; Buhro, W. E.; Loomis, R. A. Simple Surface-Trap-Filling Model for Photoluminescence Blinking Spanning Entire CdSe Quantum Wires. *J. Phys. Chem. C* **2008**, *112*, 4813–4817.
37. Galland, C.; Ghosh, Y.; Steinbruck, A.; Sykora, M.; Hollingsworth, J. A.; Klimov, V. I.; Htoon, H. Two Types of Luminescence Blinking Revealed by Spectroelectrochemistry of Single Quantum Dots. *Nature* **2011**, *479*, 203–207.
38. Park, Y.-S.; Bae, W. K.; Pietryga, J. M.; Klimov, V. I. Auger Recombination of Biexcitons and Negative and Positive Trions in Individual Quantum Dots. *ACS Nano* **2014**, *8*, 7288–7296.
39. Spinicelli, P.; Buil, S.; Quélin, X.; Mahler, B.; Dubertret, B.; Hermier, J. P. Bright and Grey States in CdSe-CdS Nanocrystals Exhibiting Strongly Reduced Blinking. *Phys. Rev. Lett.* **2009**, *102*, 136801.
40. Kuno, M.; Fromm, D. P.; Johnson, S. T.; Gallagher, A.; Nesbitt, D. J. Modeling Distributed Kinetics in Isolated Semiconductor Quantum Dots. *Phys. Rev. B* **2003**, *67*, 125304.
41. Shimizu, K. T.; Neuhauser, R. G.; Leatherdale, C. A.; Empedocles, S. A.; Woo, W. K.; Bawendi, M. G. Blinking Statistics in Single Semiconductor Nanocrystal Quantum Dots. *Phys. Rev. B* **2001**, *63*, 205316.
42. Wang, S.; Querner, C.; Emmons, T.; Drndic, M.; Crouch, C. H. Fluorescence Blinking Statistics from CdSe Core and Core/Shell Nanorods. *J. Phys. Chem. B* **2006**, *110*, 23221–23227.
43. Peterson, J. J.; Nesbitt, D. J. Modified Power Law Behavior in Quantum Dot Blinking: A Novel Role for Biexcitons and Auger Ionization. *Nano Lett.* **2009**, *9*, 338–345.
44. Stefani, F. D.; Knoll, W.; Kreiter, M.; Zhong, X.; Han, M. Y. Quantification of Photoinduced and Spontaneous Quantum-Dot Luminescence Blinking. *Phys. Rev. B* **2005**, *72*, 125304.
45. Baker, T. A.; Rouge, J. L.; Nesbitt, D. J. Single Molecule Studies of Quantum Dot Fluorescence Intermittency: Evidence for Both Dark and Light-Assisted Blinking Dynamics. *Mol. Phys.* **2009**, *107*, 1867–1878.